



Phosphorylated cellulose for water purification: a promising material with outstanding adsorption capacity towards methylene blue

Maria Hadid · Hassan Noukrati · Hicham Ben youcef · Allal Barroug · Houssine Sehaqui

Received: 12 November 2020 / Accepted: 12 June 2021 / Published online: 23 June 2021
© The Author(s), under exclusive licence to Springer Nature B.V. 2021

Abstract Enhancing the sorption properties of cellulose is a prerequisite for its efficient use in water purification as an alternative to costly activated carbon. Here, solvent-free phosphorylation of cellulose using environmentally benign and non-toxic chemicals was pursued resulting in a negatively charged material that was used to remove methylene blue (MB) from aqueous solution. Three different cellulose sources were selected, i.e., locally abundant Alfa grass, wood, and microcrystalline cellulose, with the aim to investigate the effect of the cellulose source on the functionalization degree and the removal

efficiency of methylene blue. The poor MB adsorption capacity of native cellulose ($12\text{--}40\text{ mg g}^{-1}$) reached exceptionally high values after phosphorylation ($446\text{--}705\text{ mg g}^{-1}$) resulting in one of the most promising bio-based sorbents reported up-to-date. The highest phosphorylation degree was registered on cellulose from wood conferring it with the maximum adsorption properties. Curve-fitting experimental results revealed that the adsorption data were well described by the Langmuir equation and that the pseudo-second-order kinetic represents well the interactions between cellulose and MB molecules. Finally, we show the possibility to release MB from a used sorbent when it is successively washed with phosphate ions leading to a quasi-total (97%) regeneration.

Supplementary Information The online version contains supplementary material available at <https://doi.org/10.1007/s10570-021-04012-4>.

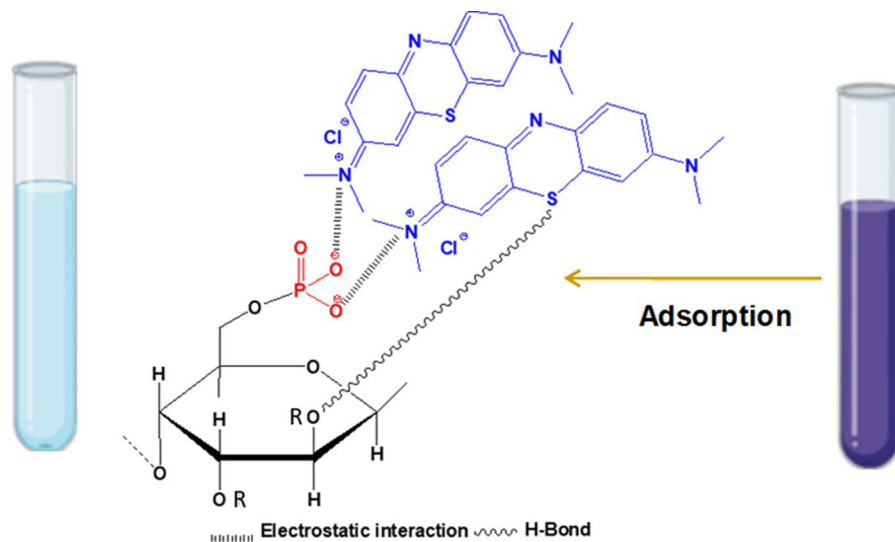
M. Hadid · H. Sehaqui (✉)
Materials Science, Energy and Nanoengineering
Department, Mohammed VI Polytechnic University
(UM6P), Lot 660 – Hay Moulay Rachid,
43150 Benguerir, Morocco
e-mail: houssine.sehaqui@um6p.ma

H. Ben youcef
High Throughput Multidisciplinary Research Laboratory,
HTMR, Mohammed VI Polytechnic University (UM6P),
Lot 660 – Hay Moulay Rachid, 43150 Benguerir,
Morocco

M. Hadid · A. Barroug
Faculty of Sciences Semlalia, Cadi Ayyad University,
40000 Marrakech, Morocco

H. Noukrati · A. Barroug
High Institute of Biological and Paramedical Sciences,
ISSB-P, Mohammed VI Polytechnic University (UM6P),
Lot 660 – Hay Moulay Rachid, 43150 Benguerir,
Morocco

Graphic abstract



Keywords Cellulose · Phosphorylation · Methylene blue · Adsorption · Adsorption kinetics · Adsorption isotherm

Introduction

Industrialization and human activities have led to an increasing number of pollutants entering water resources (Schwarzenbach et al. 2006). Amongst these, dyestuffs are full of aromatic, toxic, and hardly biodegradable chemicals thus challenging industrial wastewater treatment and hazarding the environment (Lellis et al. 2019). To satisfy demands in the textile industry alone, 10 000 different dyes amounting to some 7×10^5 tons are used each year, while partially ending up in waste stream discharges (He et al. 2013). In addition, other dye-consuming industries such as pulp and paper, pharmaceutical, and tannery are also responsible for dye discharges into the environment (He et al. 2013). This has prompted many research activities aiming to develop inexpensive, efficient, and sustainable purification technologies that could tackle dye-contaminated water (Rafatullah et al. 2010).

Adsorption seems to offer the best prospects over other water treatment methods such as coagulation and

precipitation which make use of intensive chemical treatments and results in residuals that require further treatment (Bolisetty and Mezzenga 2016). Although adsorption technologies such as activated carbon-based ones are effective and highly used for water remediation, they remain costly and difficult to regenerate, and this hampers their economical usage. Ideal alternatives would be sustainable, low-cost, high-capacity adsorbents derived from locally abundant natural substances (Han et al. 2010; Sharma et al. 2011; Gupta et al. 2013).

Cellulose, the most abundant natural polymer on earth, is undoubtedly one of the most attractive materials for designing water purification adsorbents due to its worldwide availability, renewability, benign character, facile surface modification, and processing versatility (Carpenter et al. 2015; Sehaqui et al. 2016b). To tackle the low/moderate adsorption properties of native cellulose, active functional groups are attached to its backbone allowing the immobilization of charged pollutants and non-polar species (Sehaqui 2014, 2016a, b). For instance, carboxylate or phosphate-modified cellulose filters and membranes have been effectively used for the uptake of positively charged dyes and heavy metal ions (Ma et al. 2012; Blilid et al. 2019; Lehtonen et al. 2020).

Over the past years, increased interest in cellulose phosphorylation as a promising route for the introduction of negative charges has been reborn, mainly with respect to its utilization for nanocellulose production, flame retardancy, and water purification (Ghanadpour et al. 2015; Lehtonen et al. 2020). Although cellulose phosphorylation can proceed in various media (e.g., DMF (Granja et al. 2001), DMAc/LiCl (Aoki and Nishio 2010), pyridine (Reid et al. 1949)) using various phosphorus based-chemicals [e.g., H_3PO_4 (Reid et al. 1949; Suflet et al. 2006), P_2O_5 (Granja et al. 2001), POCl_3 (Reid et al. 1949)], and at various operating conditions, the reaction with mono-ammonium and di-ammonium phosphate in the presence of urea at 150–165 °C seems to offer the best prospects as a green, simple and inexpensive route resulting in high functionalization degree and relatively low cellulose degradation. Application possibilities of phosphorylated (nano)cellulose include flame-retardancy, water purification, and many others (Noguchi et al. 2017; Ghanadpour 2018).

In the area of water purification, phosphorylated cellulose is used for its adsorption properties towards positively charged pollutants, mainly heavy metal ions and dyes. Here, the aim is to achieve similar adsorption properties to well-known commercial sorbents such as activated carbon. In a study by Sunflet et al. (2017), phosphorylated cellulose microspheres were used for the uptake of methylene blue (MB) from an aqueous solution. The microspheres displayed both a low exchange capacity of 0.24 meq g^{-1} and a low adsorption capacity towards MB (about 60 mg g^{-1}) (Suflet et al. 2017). In another study by Luo et al., phosphorylated cellulose microspheres were applied for the effective chelation of Pb^{2+} in aqueous media, and an adsorption capacity of 108 mg g^{-1} was reached (Luo et al. 2017). Srivastava et al. reported an adsorption capacity ranging from 25–70 mg g^{-1} of various metal ions (Cu^{2+} , Ni^{2+} , Cd^{2+} , Pb^{2+}) onto phosphorylated cellulose triacetate-silica composites (Srivastava et al. 2016). Oshima et al. and Zhuang et al. utilized phosphorylated bacterial cellulose as an adsorbent for metal ions and registered a good adsorption behavior for various transition metal ions, lanthanide ions, and U(VI) via ion-exchange mechanism (Oshima et al. 2008; Zhuang and Wang 2019). Phosphorylated nanocellulose paper was used to filter heavy metal ions such as Cu^{2+} from an aqueous solution, although the nanopaper's charge content

($18.6 \text{ mmol kg}^{-1}$) and the flux registered remained low (Mautner et al. 2016). Recently, Lehtonen et al. showed a great adsorption capacity of radio-active uranium species onto phosphorylated cellulose (1550 mg g^{-1}), provided by the high concentration of phosphoryl groups attached to the cellulose (1 mmol g^{-1}) (Lehtonen et al. 2020). Despite these numerous studies, the potential of phosphorylated cellulose as a promising dye adsorbent has not yet been demonstrated.

In this work, we aim to investigate the chemical characteristics and sorption properties of phosphorylated cellulose made of locally abundant resources using a straightforward phosphorylation process with diammonium phosphate/urea. A fast-growing plant thriving in dry regions of north Africa and covering a large area of about 3 million hectares in Morocco (named Alfa grass, Esparto or *Stipa tenacissima*) (El Achaby et al. 2018) has been selected as a cellulose source together with commercial wood fibers and microcrystalline cellulose. Sorption properties against methylene blue, a commonly used substance for dyeing cotton, wool and silk (Batmaz et al. 2014), and a cationic organic dye molecule extensively used in the literature as a reference adsorbate compound (Rafatullah et al. 2010), were investigated and compared to state-of-the-art sorbents reported in the literature to draw conclusions on the potential of the present biobased material for water purification. To the best of our knowledge, amongst all phosphorylated biopolymers reported to date, the present phosphorylated cellulose materials achieved unprecedented adsorption capacity against methylene blue comparable to the capacity achieved onto the best activated carbon sorbents.

Materials and methods

Dibasic ammonium phosphate ($(\text{NH}_4)_2\text{HPO}_4$), urea, KCl, NaOH, HCl, NaCl, and methylene blue (MB) were purchased from Sigma Aldrich. Microcrystalline cellulose (MCC) was purchased from Alfa Aesar. Never-dried softwood sulphite pulp fibers from Nordic Pulp and Paper (denoted wood cellulose) have a DP of 1200, lignin and hemicellulose contents of 0.7% and 13.8%, respectively. All these products were used without any prior purification.

Cellulose extraction from Alfa grass

Alfa grass (*Stipa tenacissima*) collected from the oriental region of eastern Morocco was used for cellulose extraction according to well-known alkaline and bleaching treatments. Information on the extraction process and on the properties of extracted cellulose can be found also in the publications by El Achaby et al. (Youssef et al. 2015; El Achaby et al. 2018). In brief, the original Alfa grass with a length of up to 1000 mm was first cut into 10–20 mm small fibers. These were treated in distilled water for 1 h at 60 °C followed by treatment with 4 wt% NaOH solution at 80 °C for 2 h under stirring (process repeated 3 times). A bleaching, using a solution made up of equal parts (v:v) of acetate buffer (27 g NaOH and 75 mL glacial acetic acid, diluted to 1 L of distilled water) and aqueous sodium chlorite (1.7 wt% NaClO₂ in water), was repeated 3 times to result in white-colored cellulose fibers. In these treatments, the ratio of the fibers to liquor was 1/20 (g/mL).

Phosphorylation of cellulose

10 g of cellulose was soaked in a solution containing 12 g urea, 5.1 g dibasic ammonium phosphate (NH₄)₂HPO₄, and 25 mL distilled water. The mixture was dried at 60 °C overnight and cured at 150 °C for 60 min. The modified cellulose thus obtained was thoroughly washed using distilled water, mixed in a blender for 10 min, frozen at –80 °C, and finally lyophilized under vacuum using a Cosmos freeze-dryer from Cryotec.

Materials characterization

The surface morphology of carbon-coated samples was observed using scanning electron microscopy (TESCAN-VEGA3) at an accelerating voltage of 10 kV, and the presence of phosphorus in their structure was assessed by energy dispersive X-ray analyses performed on EDAX system. X-ray diffraction analyses of the native and phosphorylated cellulose were registered in a Bruker AXS D2 PHASER system (Cu K α radiation $\lambda = 1.54060 \text{ \AA}$). The incident X-ray beam comes from a copper anticathode using radiation K α_1 ($\lambda_1 = 1.54056 \text{ \AA}$) and K α_2 ($\lambda_2 = 1.54439 \text{ \AA}$). The diffraction profiles were obtained at diffraction angles between 5 and 50°.

The crystallinity index (CI) was calculated according to the Segal method using XRD peak heights, where I_{\min} is the minimum intensity of the amorphous phase ($\sim 19^\circ$) and I_{\max} is the maximum intensity of the crystalline phase ($\sim 22.5^\circ$) (Segal et al. 1959).

$$CI(\%) = 100 \times \left(1 - \frac{I_{\min}}{I_{\max}} \right)$$

FTIR analyses of the samples were performed on a Spectrometer (PerkinElmer Frontier FTIR) equipped with an ATR reflection accessory in the range of 4000 to 400 cm⁻¹ with a resolution of 4 cm⁻¹. The phosphorus content of the phosphorylated cellulose was quantified by inductively coupled plasma optical emission spectrometry (ICP-OES), on Agilent 5110 ICP-OES Instrument. The charge content was quantified by conductometric titration (Sehaqui et al. 2014; Ghanadpour et al. 2015; Noguchi et al. 2020). The degree of substitution (DS) was calculated using the equation below wherein P% is the phosphorus percentage, 162 is the molecular weight of the anhydroglucose unit, 3100 is the atomic weight of P multiplied by 100, and 80 is the molar mass of the grafted phosphate group (Rol et al. 2020):

$$DS = \frac{162 \times P\%}{3100 - 80 \times P\%}$$

To determine the pKa of the phosphate function attached to the cellulose, the potentiometric titration was performed. Herein, the pH as a function of the added NaOH (0.1 M) was recorded. The pKa were determined from the equivalent points according to the method by Noguchi et al. (2020). The details of the potentiometric titration are given in Supplementary data S3.

The concentration of methylene blue in solution was determined by UV/VIS/NIR spectrophotometer (Perkin Elmer, Lambda 1050). The specific surface area of the native and functionalized samples was assessed by N₂ physisorption according to the Brunauer–Emmett–Teller (BET) method on a Micromeritics automated system. The samples were first degassed at 105 °C overnight prior to the analysis followed by N₂ adsorption at –196 °C over a relative vapor pressure of 0.01–0.3.

Adsorption experiments

The retention capacity of methylene blue on native and phosphorylated cellulose was examined by the batch method at room temperature (ca. 25 °C). Freshly prepared synthetic solutions have been obtained by dissolving the appropriate amount of MB in a standard potassium chloride solution (KCl) with a given concentration (1 mM) and at a pH value close to 7. The latter was adjusted using nitric acid and ammonium hydroxide. Adsorption experiments were performed in polyethylene tubes with a capacity of 10 ml. Thus, 10 mg of the sorbent were placed in 10 ml of the MB solution and sonicated for 1 min. Suspensions were then incubated for a specific period of time, and thereafter separated from the adsorbent by centrifugation at 15,000 rpm for 10 min.

For the kinetic experiments, the initial concentration of MB solutions was fixed at 10 mg L⁻¹ (Native Alfa and MCC), 20 mg L⁻¹ (Native wood), 500 mg L⁻¹ (phosphorylated Alfa), and 800 mg L⁻¹ (phosphorylated MCC and Wood). Adsorption experiments aiming to establish the adsorption isotherm of MB onto cellulose were performed as stated above with MB concentrations in the range of 20–300 mg L⁻¹ and 50–1000 mg L⁻¹, respectively for native and phosphorylated cellulose. The suspensions were incubated for 2 h for the former and 4 h for the latter specimens ensuring the equilibrium condition is satisfied.

Suspension of sorbent in KCl medium without MB incubated similarly to the adsorption tests were used as controls. The pH of the suspensions measured before and after adsorption indicated that the variation was found to be in the range 6.4–7.2. In parallel with the performed adsorption experiments, blank tests containing only MB solutions covering the range of concentrations investigated without the presence of cellulose were performed under the same conditions cited earlier. The amount of MB molecules adsorbed was determined from the difference in the concentration between the blank and the supernatant of the suspensions.

After centrifugation, the supernatant concentration was determined by UV/VIS spectrophotometry at the wavelength corresponding to the maximum

absorbance of MB solution ($\lambda = 664$ nm) using calibration curves established with known MB concentrations. MB calibration curve is given in Supplementary data S1. The adsorbed amount (Q_{ads}) and the percentage adsorbed of MB by the cellulosic sorbent (removal efficiency) were calculated using the following formulas:

$$Q_{ads} = \frac{(C_0 - C_e)}{m} \times V \quad (1)$$

$$Removal\ efficiency(\%) = \frac{(C_0 - C_e)}{C_0} \times 100 \quad (2)$$

where C_0 (mg L⁻¹) is the initial dye concentration, C_e (mg L⁻¹) may stand for the dye concentration at a given time or at equilibrium, V (mL) is the volume of the solution, and m (mg) is the amount of adsorbent used.

Adsorption tests were performed several times to estimate the error percentage emanating from the volume uptake, weighing, and dilution on the amount of MB adsorbed onto the cellulose. This percentage was found to be 6% for native and phosphorylated cellulose.

Desorption test/Regeneration of the adsorbent

Desorption was carried out on phosphorylated cellulose from Alfa grass at room temperature (ca. 25 °C) with respect to dilution. First, adsorption tests were performed as cited earlier with a methylene blue concentration of 50–150 mg L⁻¹ (located in the rising part of the isotherms), and the amounts adsorbed were determined. The suspension obtained after adsorption was centrifuged and the supernatant (95%) was removed and replaced by the same volume of a solution of 1 mM potassium chloride. The deposit was re-dispersed and incubated for 4 h to reach new equilibrium conditions. The suspension obtained was again centrifuged and the supernatant was removed and analyzed giving the amount of MB desorbed (Q_{des}) from which the percent desorbed was determined as:

$$Dye\ desorbed(\%) = \frac{Q_{des}}{Q_{ads}} * 100 \quad (3)$$

This operation was repeated six times on the same sample.

The desorption test in the presence of added phosphate ions was also performed as described above using a 1 mM aqueous potassium chloride solution containing dibasic ammonium phosphate ($(\text{NH}_4)_2\text{HPO}_4$) at a concentration of 25 mM or 50 mM (pH \sim 7.5).

Results and discussion

Characterization of the adsorbent

SEM micrographs of native and phosphorylated cellulose fibers are displayed in Fig. 1. The morphology of the cellulose sorbent does not seem to undergo significant changes after phosphorylation. Alfa fibers exhibit a high aspect ratio with a diameter of 5–10 μm and a rather spherical cross-section. The fibers from wood are flatter with a lateral dimension of ca. 20–30 μm . Cellulose from MCC exhibits flakes-like morphology with short aspect ratio fibers characteristic of the acid hydrolysis treatment used for the preparation of this material. As expected from their relatively large diameter, the specific surface area of all these materials measured in the dry state is low (below 2 $\text{m}^2 \text{g}^{-1}$; see Table 1). Nevertheless, we have shown in our previous work that in the presence of moisture (using water vapor as adsorbate), the surfaces of cellulose nanofibrils becomes available for sorption leading to a specific surface area of a few hundred $\text{m}^2 \text{g}^{-1}$ (Sehaqui et al. 2016b).

Alfa cellulose was selected to qualitatively examine the surface composition of native and phosphorylated samples by Energy-dispersive X-ray (EDX) spectroscopy. Native cellulose analysis shows the presence of carbon and oxygen elements at their corresponding binding energies around 0.2 and 0.5 keV, respectively (Fig. 2a). Phosphorylated cellulose analysis shows the presence of an additional peak of phosphorus element at around 2 keV (Fig. 2b).

To assess the effect of the phosphorylation reaction on the crystallinity of cellulose, X-ray diffraction (XRD) analyses were performed. Spectra of native and phosphorylated samples presented in Fig. 3 display the same peaks at 2θ angles of 16.6°, 22.3°, and 34.4°, corresponding to (110), (200), and (004) lattices, respectively, characteristic of the cellulose I structure (French 2014). This confirms that the present

phosphorylation of cellulose is heterogeneous and occurs mainly at the surface of the crystallites without total cellulose dissolution. The crystallinity index (CI) of various cellulose samples determined according to the Segal method is given in Table 1. Native cellulose from wood has the least CI of 61% versus a CI of 76% and 77% for Alfa cellulose and MCC, respectively. After phosphorylation, the CI decreases to values of 55–62%, and this might be attributed to a partial ‘disorder’ of the phosphorylated cellulose at the surface of the fibrils. In the study by Noguchi et al. on phosphorylation using ammonium phosphate, the CI of cellulose from softwood pulp was not altered by the reaction wherein a maximum curing time of 10 min was used (Noguchi et al. 2017). A small decrease in the CI from 75 to 67% was observed in the study by Rol et al. using dibasic ammonium phosphate at similar drying temperature and time used herein (Rol et al. 2020).

We further subjected the samples to FTIR analysis. Selected spectrum of Alfa cellulose in Fig. 4 shows characteristic bands of cellulose, namely at 3370–3250 cm^{-1} corresponding to the stretching vibrations of C-H and OH functional groups, at 1159 cm^{-1} corresponding to C–O–C asymmetric stretching of the cellulose, and at 1033 cm^{-1} attributed to the C–O–C pyranose ring skeletal vibration (El Achaby et al. 2018). For the phosphorylated sample, the analysis revealed the appearance of new peaks at 1231 and 921 cm^{-1} characteristics of the stretching of the P = O and P-OH bonds, at 830 cm^{-1} corresponding to the P-O-C bond, and at 1732 cm^{-1} corresponding to the C = O stretching mode (Ghanadpour et al. 2015). The C = O bond, which is not observed in native cellulose, attests to the phosphorylation-induced oxidation of the fibers, in agreement with works reported by Ghanadpour et al. wherein the peak at ca. 1730 cm^{-1} was also observed by FTIR and confirmed by XPS (Ghanadpour et al. 2015). A proposed structure of phosphorylated cellulose is shown in Scheme 1, while other possible structures can be found elsewhere (Božič et al. 2014). Due to their hydrophilic character, OH bending vibration characteristic of sorbed water appears in the FTIR spectra of pure and phosphorylated materials as a band/shoulder at 1640 cm^{-1} (Célineo et al. 2014).

The P content of phosphorylated samples ranges from 1.85 to 2.64 mmol g^{-1} (Table 1). The highest

value is registered for the least crystalline cellulose (from wood), and this is expected since phosphorylation occurs preferentially in the “amorphous” regions of cellulose. A maximum P content of 2.2 mmol g⁻¹ was obtained in the aforementioned study by Noguchi et al. (Noguchi et al. 2017).

Phosphate groups introduced to cellulose enhances its negative charges and govern its adsorption properties towards basic pollutants via electrostatic interactions. The charge content was evaluated by conductometric titration and ranges from 3.8–4.7 mmol g⁻¹ (Table 1 and supplementary data S2) and compares well with the 2.93–4.40 mmol g⁻¹ range registered in the study by Rol et al. wherein dibasic ammonium phosphate was used for cellulose phosphorylation (Rol et al. 2020). Ghanadpour et al. registered a much lower charge content of 1.8 mmol g⁻¹, yet the phosphorylated cellulose displayed excellent flame-retardancy (Ghanadpour et al. 2015). From phosphorylated cellulose structure, we expect that each P atom can give a maximum of two negative charges (Scheme 1), while the presence of carboxylate groups is also contributing to the total charges of the

phosphorylated cellulose (see FTIR results). Interestingly, the charge content of phosphorylated cellulose is much higher than the one registered for TEMPO-oxidized cellulose from various origins (0.52–1.69 mmol g⁻¹) (Okita et al. 2010).

In agreement with other work (Ait Benhamou et al. 2021), the conductometric titration graph shows three distinctive inflexion points (Supplementary data S2) characteristics of:

- The consumption of the strong acid (HCl) and the beginning of titration of the first weak acid of the phosphate function.
- The titration of the second weak acid of the phosphate function.
- The consumption of all weak acids of the phosphate and the beginning of NaOH excess.

The presence of three inflection points indicates that two hydroxyl groups have been consumed during the titration process, in agreement with pKa results wherein two acidities were detected (see later discussion), and in agreement with our recently published work (Ait Benhamou et al. 2021).

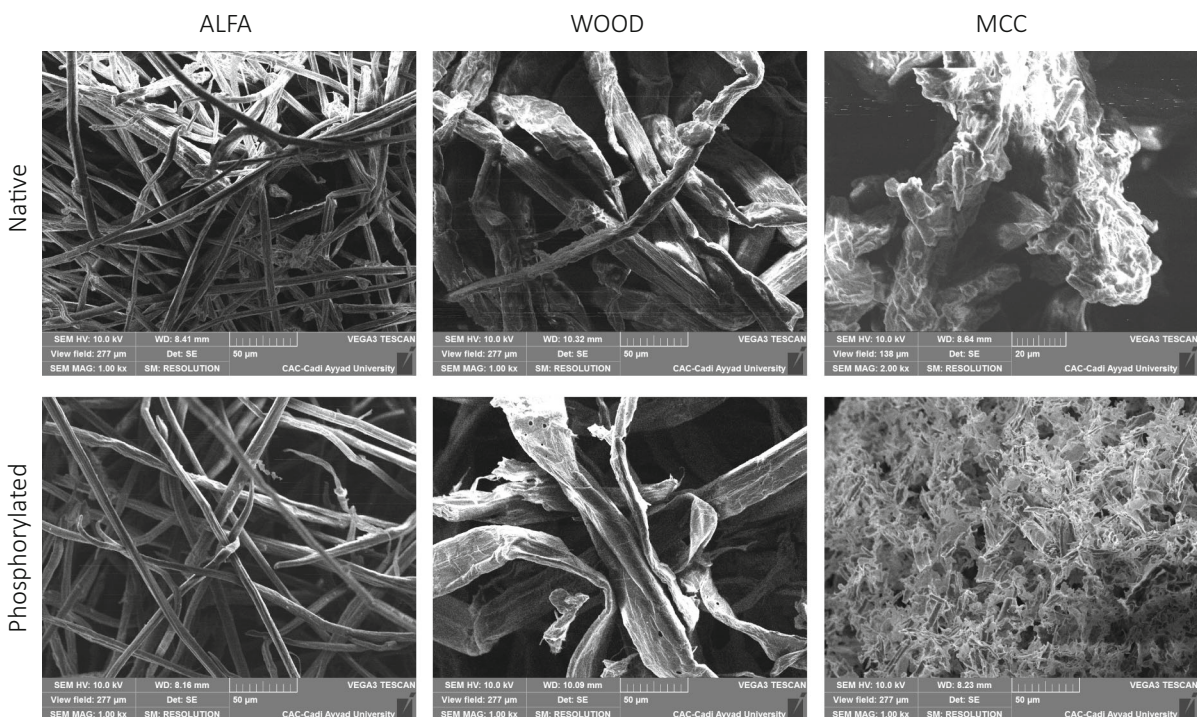


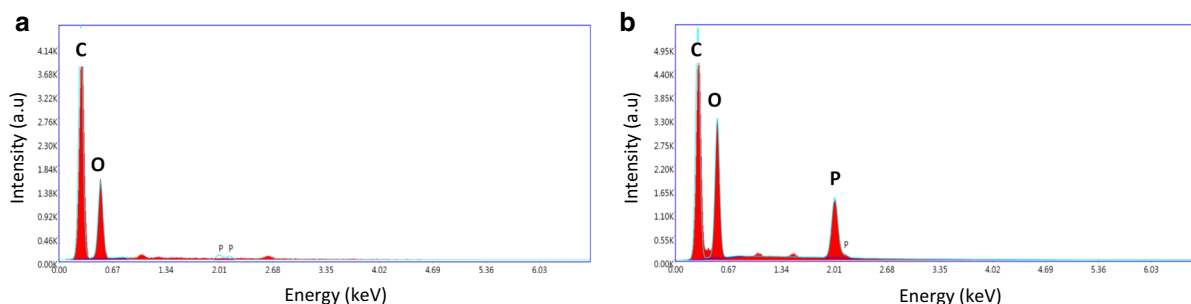
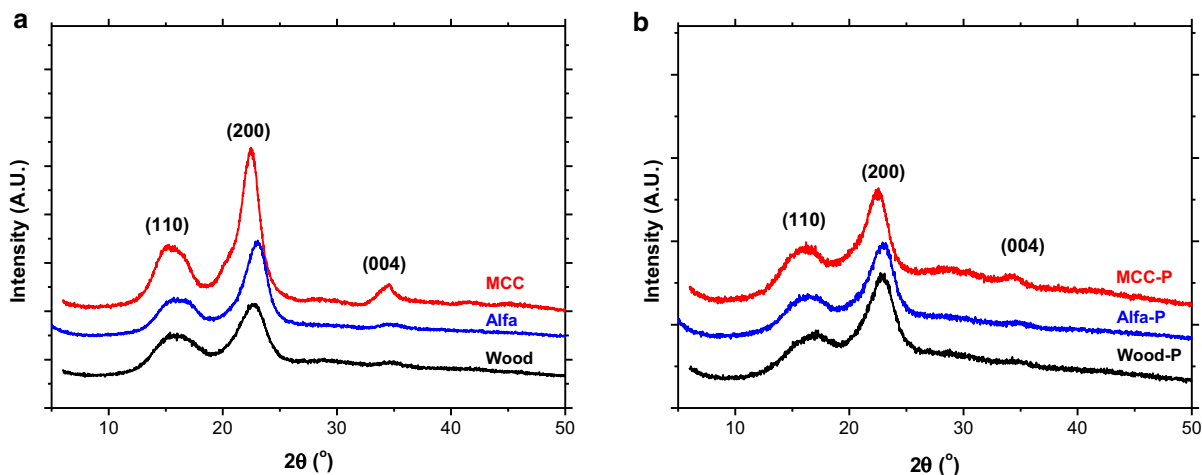
Fig. 1 SEM images of native and phosphorylated cellulose

Table 1 Characteristics of native and phosphorylated cellulose: crystallinity index, Phosphorus content, charge content and degree of substitution. The index “-P” refers to phosphorylated materials

	Wood	Wood-P	MCC	MCC-P	Alfa	Alfa-P
Crystallinity index (%)	61	58	77	55	76	62
Phosphorus content (mmol g ⁻¹)	a	2.64	a	2.23	a	1.85
Charge content (mmol g ⁻¹)	b	4.6	b	4.7	b	3.8
Degree of substitution (DS)	–	0.54	–	0.44	–	0.35
BET specific surface area (m ² g ⁻¹)	0.4	1.2	1.0	1.9	0.8	0.8

^aBelow the detection limit (0.161 μmol g⁻¹)

^bNot available

**Fig. 2** EDX spectra of (a) native and (b) phosphorylated cellulose from Alfa**Fig. 3** XRD spectra of (a) native and (b) phosphorylated cellulose

The potentiometric titration curve registered for phosphorylated cellulose from Alfa indicates pKa values of the phosphate function of 2.98 and 7.65, in agreement with pKa values of phosphorylated cellulose reported to be 3.1 and 8.3 by Noguchi et al. (Noguchi et al. 2020).

The resulting bulk degree of substitution (DS) of the present phosphorylated cellulose lies within 0.35 and 0.54 and can be considered very high. The DS, like the phosphorus content, is associated with the crystallinity of the neat cellulose. Lower CI values of the latter are expected to give higher DS since the

phosphorylation is promoted in the amorphous zones of cellulose. DS between 0.18 and 0.45 have been found in the study by Rol et al. by the same calculation method used herein (Rol et al. 2020). The use of XPS to evaluate the DS allows estimating the substitution due to phosphorylation and carboxylation. Here, $DS_{\text{phosphate}}$ of 0.014–0.047 and $DS_{\text{carboxylate}}$ of 0.024–0.050 were found for a total charge content between 0.56–1.84 mmol g^{-1} (Ghanadpour et al. 2015).

Sorption rate

The time of contact between MB and cellulose which is required to reach equilibrium was determined at room temperature. Figure 5 illustrates the evolution of the quantity of MB adsorbed at room temperature on native and phosphorylated cellulose as a function of the incubation time.

As can be seen, the adsorption of MB onto the cellulose sorbent is a fast process. The equilibrium is reached in less than 15 min of contact between the sorbent and the sorbate (Fig. 5a). However, a relatively longer equilibrium time of about 1 h is needed for MB adsorption onto phosphorylated cellulose (Fig. 5b). In comparison to the uptake of MB by activated carbon which necessitates an equilibrium time of 6 to 24 h (Hameed et al. 2007), the present adsorption process is much faster under the investigated conditions. Also, the kinetic of MB uptake onto phosphorylated cellulose presented herein is faster compared to the kinetic of MB uptake onto

phosphorylated cellulose microspheres that requires between 100–400 min to reach equilibrium at MB dosages of 100–500 mg L^{-1} (Suflet et al. 2017). This is likely related to the high charge content of the present functionalized materials.

Modeling kinetic data is based on mathematical laws that describe the relationship between the time of contact (t) and the quantity adsorbed on the material at this time (Q_t). In this study, the kinetic data were fitted to the pseudo-first-order (Lagergren) and pseudo-second-order kinetic models (Eqs. (4) and (5), respectively) commonly used to investigate the nature of the interaction between adsorbent/adsorbate systems (Azizian 2004):

$$\ln(Q_e - Q_t) = \ln Q_e - k_1 t \quad (4)$$

$$\frac{t}{Q_t} = \frac{1}{k_2 Q_e^2} + \frac{t}{Q_e} \quad (5)$$

In these equations, Q_e (mg L^{-1}) and Q_t (mg L^{-1}) represent respectively the quantities of MB adsorbed at equilibrium and at a time of contact t . k_1 (min^{-1}) and k_2 ($g \text{ mg}^{-1} \text{ min}^{-1}$) are the constants of the Lagergren and pseudo-second-order, respectively.

Referring to Eq. (4), the graph representing “ $\ln(Q_e - Q_t)$ ” as a function of “ t ” should be linear so that the corresponding model is applicable. However, the data points of the examined sorbents were not well fitted to this equation; thus, the correlation coefficients obtained were low ($0.078 < R^2 < 0.890$) as indicated in Table 2 and Fig. 6a. Consequently, the experimental results do not conform to this model.

On the other hand, the data of the linearized form of the kinetics according to the pseudo-second-order model gave a high correlation coefficient ($0.992 < R^2 < 0.999$; see Table 2 and Fig. 6b), and Q_e data approached experimental values Q_{exp} (see Table 2). This indicates that the uptake of MB molecules by native and phosphorylated cellulose follows the pseudo-second-order model. Thus, it can be said that the dye retention rate was controlled by chemisorption, including valence forces by sharing or exchange electrons between MB and cellulose. Pseudo-second order kinetic was also observed for the adsorption of methylene blue onto activated carbon (Hameed et al. 2007), metallic organic frameworks (Haque et al. 2011), and nanocrystalline cellulose (He et al. 2013).

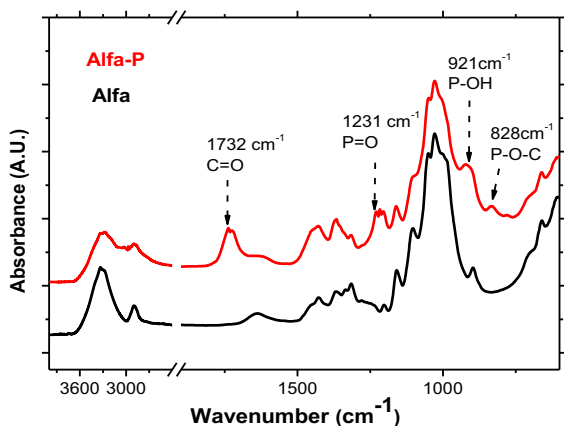
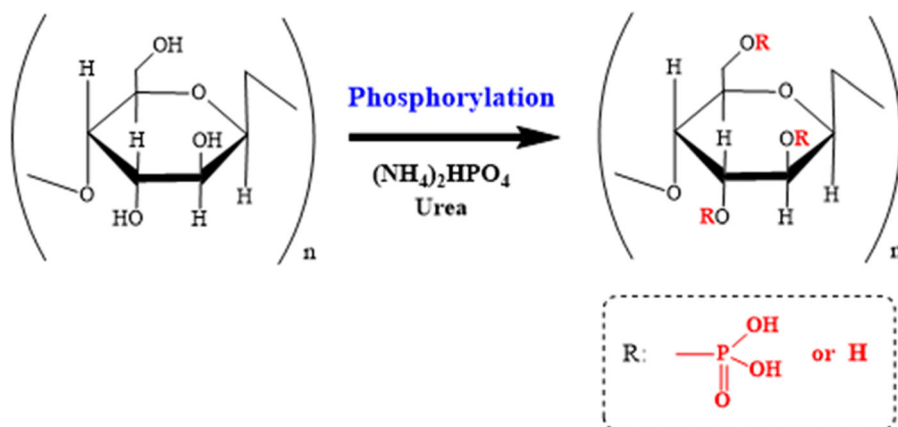


Fig. 4 FTIR spectra of native and phosphorylated cellulose from Alfa



Scheme 1 Suggested structure of phosphorylated cellulose

Adsorption isotherm

Adsorption experiments for native and phosphorylated substrates were performed at room temperature with MB concentration in the range of 20–300 mg L⁻¹ and 50–1000 mg L⁻¹, respectively for native and phosphorylated cellulose. The isotherms represent the evolution of the amount of MB adsorbed as a function of its remaining concentration in solution at equilibrium (Fig. 7).

From Fig. 7b, it can be seen that the maximum amount adsorbed was reached at a low equilibrium concentration of MB after which it remained quasi-constant, indicating a high adsorption-adsorbate affinity. Such high affinity was not observed for the native cellulose samples (Fig. 7a). MB adsorption capacity onto these latter reaches a maximum of ~ 40 mg g⁻¹ for wood cellulose and ~ 10 mg g⁻¹ for Alfa cellulose and MCC. The presence of more “amorphous” chains in wood cellulose is seemingly responsible for its higher adsorption capacity as MB cannot access the crystallites (see crystallinity index values in Table 1). Nevertheless, the values registered for all native cellulose materials remain low, and this is mainly due to the absence of highly active groups (e.g. phosphates and/or carboxylates) on their structure. In contrast, a substantial amount of phosphates introduced to cellulose results in a 15–60 fold increase in their MB adsorption capacity reaching 450–695 mg g⁻¹. The adsorption capacity of these sorbents correlates well with their phosphorus and charge contents as phosphorylated cellulose from wood has the highest

MB adsorption capacity, while phosphorylated cellulose from Alfa has the least. Apart from the charge and P contents, the difference in the amount of MB adsorbed may also be related to the crystallinity of the samples, as MB has easier access to the amorphous zones of cellulose. As compared with phosphorylated cellulose microspheres displaying a MB adsorption capacity of 58.8 mg g⁻¹, our functionalized sorbents have tenfold higher adsorption capacity which is attributed to their much higher charge content of 3.8–4.7 mmol g⁻¹ in comparison to the low exchange capacity of 0.24 meq g⁻¹ of the phosphorylated cellulose microspheres (Sufflet et al. 2017). Even nanocrystalline cellulose with a degree of oxidation of 0.10 and a surface area as high as 272 m² g⁻¹ has an adsorption capacity towards MB of 101 mg g⁻¹.

Moreover, adsorption capacities obtained for various phosphorylated cellulose were compared to the adsorption capacity of over 170 sorbents reported in the review article by Rafatullah et al. (Rafatullah et al. 2010), and the results are schematized in Supplementary data S4 and briefly discussed herein:

- Most commercial activated carbon and coal materials have a MB adsorption capacity in the 200–400 mg g⁻¹ range. The present phosphorylated cellulose performs better in terms of MB adsorption capacity than ~ 95% of the commercial activated carbon and coal materials.
- Activated carbons derived from agricultural and industrial wastes have a scattered adsorption capacity between 1–486 mg g⁻¹, which can be

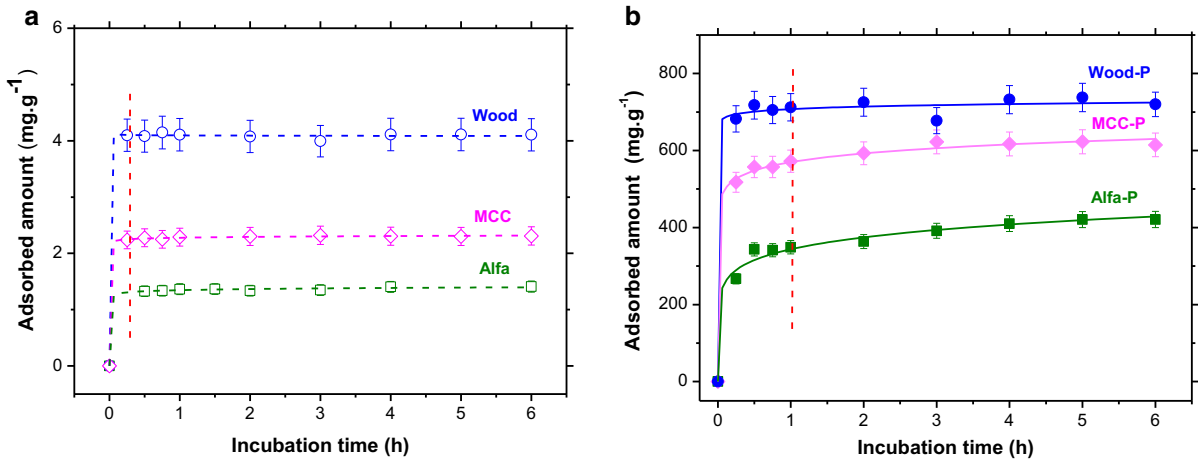


Fig. 5 Evolution of the adsorbed amount of MB as a function of incubation time for (a) native and (b) phosphorylated cellulose

explained by the various raw materials and activation conditions used for the preparation of such sorbents. The present phosphorylated cellulose performs better in terms of MB adsorption capacity than ~ 98% of the activated carbons derived from agricultural and industrial wastes.

- Although natural materials (unmodified) such as clay minerals are attractive in terms of their low cost and abundance, their sorption properties are moderate and lie mostly in the range 1–200 mg g⁻¹. Montmorillonite displays the highest MB adsorption capacity of ~ 300 mg g⁻¹, which is about half the value registered for the present phosphorylated cellulose.
- Most bioadsorbents have a MB adsorption capacity in the 1–300 mg g⁻¹ range. Bioadsorbents based on chemically modified biomass such as

poly(methacrylic acid) and poly(amic acid) modified biomass of baker’s yeast offer the best performance of 870 and 680 mg g⁻¹, respectively. This confirms the promises of this type of materials wherein the present phosphorylated cellulose can be categorized as one the best reported.

- Agricultural solid wastes are available in large quantities and low cost, and have a MB adsorption capacity mostly in the range 1–400 mg g⁻¹. 2% of these materials, namely, Teak wood bark, Papaya seeds, and Grass waste, are reported to have a MB adsorption capacity surpassing that registered for the present phosphorylated cellulose.
- Industrial solid wastes have a MB adsorption capacity in the 0.5–250 mg g⁻¹ range, and may not be an efficient option for dye-contaminated water

Table 2 Pseudo-first and second-order kinetic parameters of MB adsorption onto cellulose

Sorption models	Parameters	Alfa	Alfa-P	MCC	MCC-P	Wood	Wood-P
Experimental	Q _{exp} (mg g ⁻¹)	1.4	420	2.3	635	4.1	615
Pseudo-first order	K ₁ (min ⁻¹)	0.003	0.011	0.013	0.007	0.005	0.015
	Q _e (mg g ⁻¹)	0.40	30.5	7.6	9.1	0.31	125.8
	R ²	0.555	0.890	0.622	0.555	0.078	0.766
Pseudo-second order	K ₂ (g.mg ⁻¹ min ⁻¹)	0.162	7.4 × 10 ⁻⁵	0.303	6.2 × 10 ⁻⁴	0.497	3.6 × 10 ⁻⁴
	Q _e (mg g ⁻¹)	1.4	457	2.3	639	4.1	627
	R ²	0.998	0.992	0.999	0.999	0.999	0.999

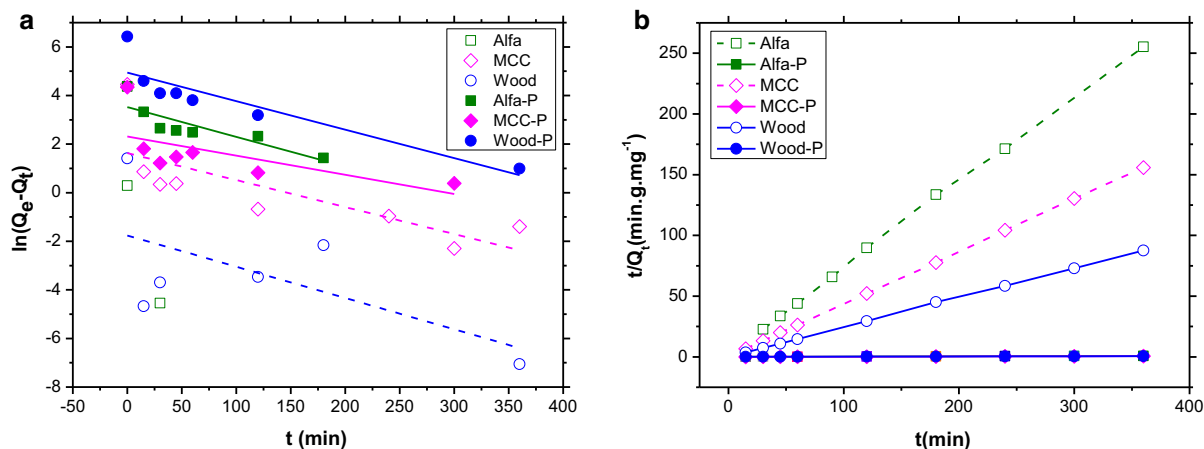


Fig. 6 Plots showing (a) $\ln(Q_e - Q_t)$ and (b) t/Q_t as a function of time. Please note that in Fig. 6.b, the graphs of the Alfa-P, MCC-P and Wood-P overlaps

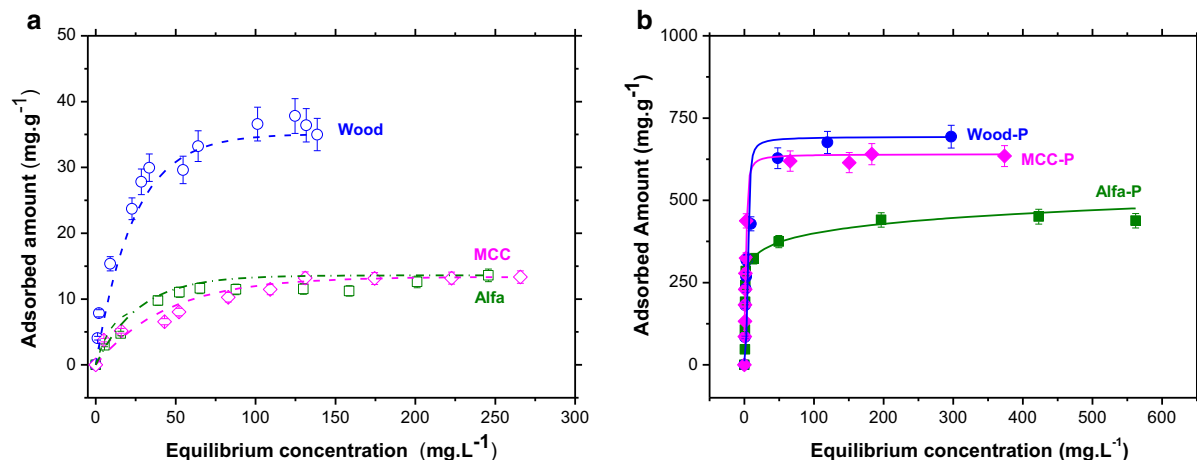


Fig. 7 Adsorption isotherms of MB onto (a) native and (b) phosphorylated cellulose: Evolution of the amount adsorbed of MB as a function of its remaining concentration in solution at equilibrium (equilibrium concentration)

treatment compared to the proposed materials herein.

To elucidate the interaction between cellulose and MB, the Langmuir equation given by Eq. 6 has been tested with the experimental results. The linearized form of this equation was considered (Eq. 7), and the evolution of “ C_e/Q_{ads} ” as a function of “ C_e ” was plotted (see Fig. 8).

$$Q_{ads} = N \frac{KC_e}{1 + KC_e} \quad (6)$$

$$\frac{C_e}{Q_{ads}} = \frac{1}{N} C_e + \frac{1}{KN} \quad (7)$$

where Q_{ads} is the amount of MB molecules adsorbed, C_e the equilibrium concentration, N the maximum amount adsorbed, and K the affinity constant.

As shown in Fig. 8, a linear relationship was found with correlation coefficients of 0.973–0.997 for native cellulose and 0.999 for phosphorylated ones. This indicates that the adsorption isotherms complies with the Langmuir type which assumes monolayer coverage of adsorbate over a homogeneous adsorbent surface where each molecule adsorbed reversibly onto its surface requires equal adsorption activation energy (Kannan and Sundaram 2001). Possible interactions between MB molecules and phosphorylated cellulose are represented in Supplementary data S5.

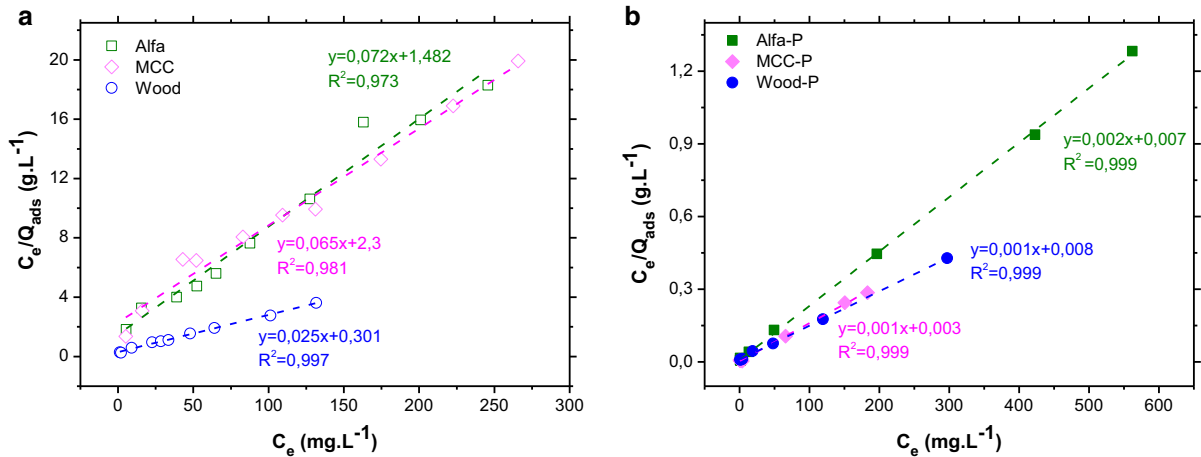


Fig. 8 The evolution of C_e/Q_{ads} as a function of C_e for (a) native, and (b) phosphorylated cellulose

Table 3 Langmuir adsorption parameters of MB onto native and phosphorylated cellulose: affinity constant (K) and maximum amount adsorbed (N)

Langmuir parameters	Alfa	Alfa-P	MCC	MCC-P	Wood	Wood-P
N (mg g ⁻¹)	12.3 ± 0.7	446 ± 27	15.3 ± 0.9	639 ± 38	39.6 ± 2.4	704 ± 42
K (L mg ⁻¹)	0.09 ± 0.006	0.29 ± 0.02	0.028 ± 0.002	0.39 ± 0.02	0.080 ± 0.005	0.21 ± 0.01
R ²	0.973	0.999	0.981	0.999	0.997	0.999

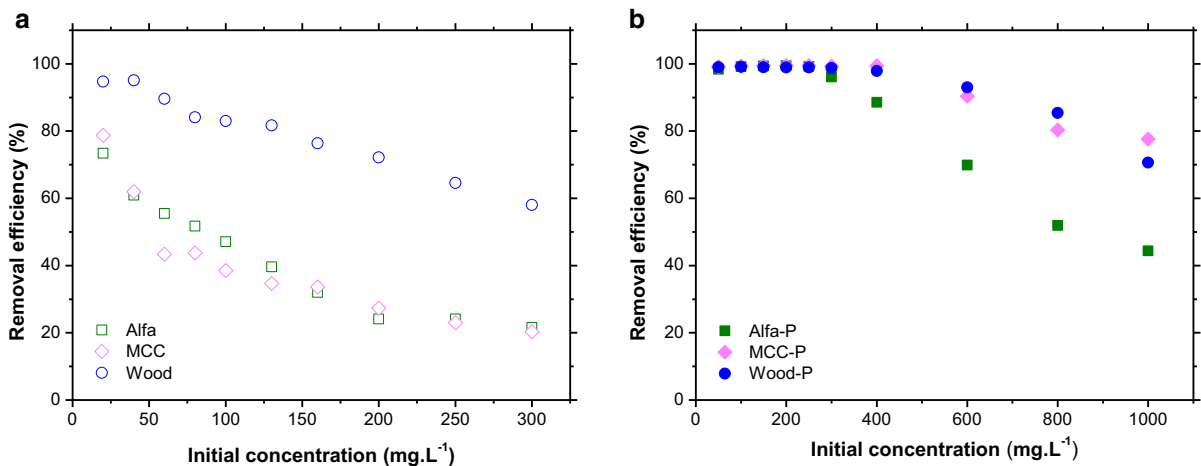


Fig. 9 Removal efficiency of MB as a function of initial concentration

The characteristic parameters of the adsorption, namely the amount adsorbed at saturation (N) and the apparent affinity constant of the adsorbate for the surface of the solid (K), were determined from the Langmuir linearized equation (Eq. 7) and are grouped in Table 3. Clearly, phosphorylation of cellulose

enhanced both the amount adsorbed at saturation and the apparent affinity of MB to the sorbent surface.

The MB removal efficiency of native and phosphorylated sorbents are given in Fig. 9. Native cellulose from Alfa and MCC shows poor MB removal percentage below 80% for all initial concentrations

of MB tested herein. Native cellulose from wood performs better removing 95% of MB at initial concentrations below 40 mg L⁻¹. Yet the % of MB removed falls below 80% for initial MB concentrations above 130 mg L⁻¹. On the other hand, phosphorylated cellulose permits the efficient removal of ~ 99% of MB up to an initial MB concentration of 250–400 mg L⁻¹, which is higher than the 10–200 mg L⁻¹ dye concentration encountered in industrial wastewater (Sivaram et al. 2018). Hence, the present phosphorylated cellulose sorbents have outstanding overall performance as they combine fast adsorption kinetic, high adsorption capacity, and good removal efficiency.

Regeneration of the sorbent

First, the desorption of MB attached to phosphorylated cellulose from Alfa has been investigated by using fresh KCl solutions at 1 mM. For an initial MB concentration of 50–150 mg L⁻¹ (used for adsorption), a negligible MB desorption of 1.9–2.4% was registered after 6 cycles (Fig. 10), attributed to the difficulty of simultaneously breaking all the bonds involved in the adsorption process. On the other hand, the use of 25 mM and 50 mM phosphate ions afforded a much higher amount of MB desorbed, i.e., 50–84% and 75–97%, respectively. As expected, higher phosphate ions concentration in the medium promotes the desorption process since they compete with the phosphate groups attached to the cellulose for the adsorbing site of MB. Moreover, there is an inverse displacement of MB molecules from low to high phosphate concentration regions.

It is interesting to note that the desorbed percentage is higher for lower MB concentration (used for

adsorption). Hence, for a MB concentration of 50 mg L⁻¹, a quasi-total liberation of MB (93%) was registered already at the 4th ‘washing’ cycle, and then remained quasi-constant for the subsequent cycles reaching 97% in the 6th cycle (Fig. 10a). Another remark is that all curves are linear so that the incremental percent of MB desorbed is nearly the same for each cycle. The increment goes from 8–14% for a phosphate concentration of 25 mM to 12–23% for a phosphate concentration of 50 mM. Hence, concentrated phosphate ions could be effectively used for the regeneration of the exhausted cellulose sorbents for their multiple utilization, towards efficient and environmentally benign utilization of these biobased materials.

Conclusion

Methylene blue has been selected to investigate the sorption properties of native and phosphorylated cellulose towards positively charged contaminants. In its native form, cellulose lacks highly acidic functions and shows a poor MB adsorption capacity of 10–40 mg g⁻¹. Affinity towards MB is enhanced after grafting phosphates to cellulose from various origins, reaching adsorption capacities of 446–705 mg g⁻¹ at phosphorus contents of 1.85–2.64 mmol g⁻¹. The reason is the presence of the negatively charged phosphate groups in the phosphorylated materials which attract the functional groups of MB molecules via electrostatic interactions. Comparison with data from the literature indicates that the present phosphorylated cellulose has a faster kinetic of MB adsorption than what is reported for activated carbon, as well as a MB adsorption capacity

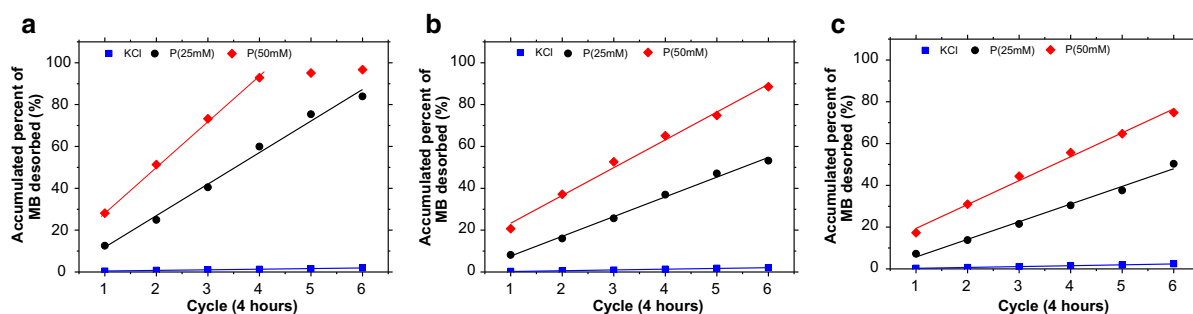


Fig. 10 MB desorption from phosphorylated Alfa cellulose using 1 mM KCl or phosphate solutions. The initial MB concentrations used for adsorption are (a) 50 mg L⁻¹, (b) 100 mg L⁻¹ and (c) 150 mg L⁻¹

surpassing that of ~ 98% reported sorbents, including activated carbon, natural materials, bioadsorbents, and agricultural wastes. The outstanding performance of the present sorbent together with its facile preparation, eco-friendly character, and regeneration possibility make it a promising water purification material.

Acknowledgments UM6P and Cadi Ayyad colleagues, namely, Mounir El Achaby, Youssef Tamraoui, Toufik Elmehdi, Ayoub Ouarga, Soumia Boukind and Hamid Ait Said, are thanked for their assistance for materials analyses. The authors would also like to thank the Center of Analysis and Characterization (CAC) of Cadi Ayyad University for SEM-EDX characterization.

Declarations

Conflict of interest The authors declare that they have no conflict of interest.

Ethical approval The article does not include human participants and/or animals research.

Informed consent Informed consent was obtained from all participants.

References

- Ait Benhamou A, Kassab Z, Nadifiyine M et al (2021) Extraction, characterization and chemical functionalization of phosphorylated cellulose derivatives from Giant Reed Plant. *Cellulose* 1:1–18. <https://doi.org/10.1007/s10570-021-03842-6>
- Aoki D, Nishio Y (2010) Phosphorylated cellulose propionate derivatives as thermoplastic flame resistant/retardant materials: Influence of regioselective phosphorylation on their thermal degradation behaviour. *Cellulose* 17:963–976. <https://doi.org/10.1007/s10570-010-9440-8>
- Azizian S (2004) Kinetic models of sorption: A theoretical analysis. *J Colloid Interface Sci* 276:47–52. <https://doi.org/10.1016/j.jcis.2004.03.048>
- Batmaz R, Mohammed N, Zaman M et al (2014) Cellulose nanocrystals as promising adsorbents for the removal of cationic dyes. *Cellulose* 21:1655–1665. <https://doi.org/10.1007/s10570-014-0168-8>
- Bllid S, Katir N, El Haskouri J et al (2019) Phosphorylated micro- vs. nano-cellulose: a comparative study on their surface functionalisation, growth of titanium-oxo-phosphate clusters and removal of chemical pollutants. *New J Chem* 43:15555–15562. <https://doi.org/10.1039/c9nj03187a>
- Bolisetty S, Mezzenga R (2016) Amyloid-carbon hybrid membranes for universal water purification. *Nat Nanotechnol* 11:365–371. <https://doi.org/10.1038/nnano.2015.310>
- Božić M, Liu P, Mathew AP, Kokol V (2014) Enzymatic phosphorylation of cellulose nanofibers to new highly-ions adsorbing, flame-retardant and hydroxyapatite-growth induced natural nanoparticles. *Cellulose* 21:2713–2726. <https://doi.org/10.1007/s10570-014-0281-8>
- Carpenter AW, De Lannoy CF, Wiesner MR (2015) Cellulose nanomaterials in water treatment technologies. *Environ Sci Technol* 49:5277–5287. <https://doi.org/10.1021/es506351r>
- Céline A, Gonçalves O, Jacquemin F, Fréour S (2014) Qualitative and quantitative assessment of water sorption in natural fibres using ATR-FTIR spectroscopy. *Carbohydr Polym* 101:163–170. <https://doi.org/10.1016/j.carbpol.2013.09.023>
- El Achaby M, Kassab Z, Barakat A, Aboulkas A (2018) Alfa fibers as viable sustainable source for cellulose nanocrystals extraction: Application for improving the tensile properties of biopolymer nanocomposite films. *Ind Crops Prod* 112:499–510. <https://doi.org/10.1016/j.indcrop.2017.12.049>
- French AD (2014) Idealized powder diffraction patterns for cellulose polymorphs. *Cellulose* 21:885–896. <https://doi.org/10.1007/s10570-013-0030-4>
- Ghanadpour M (2018) Phosphorylated cellulose nanofibrils: a nano-tool for preparing cellulose-based flame-retardant materials. PhD Thesis. KTH—Stockholm
- Ghanadpour M, Carosio F, Larsson PT, Wågberg L (2015) Phosphorylated Cellulose Nanofibrils: A Renewable Nanomaterial for the Preparation of Intrinsically Flame-Retardant Materials. *Biomacromol* 16:3399–3410. <https://doi.org/10.1021/acs.biomac.5b01117>
- Granja P, Poullységu L, Pétraud M et al (2001) Cellulose phosphates as biomaterials. I. Synthesis and characterization of highly phosphorylated cellulose gels. *J Appl Polym Sci* 82:3341–3353. <https://doi.org/10.1002/app.2193>
- Gupta VK, Agarwal S, Singh P, Pathania D (2013) Acrylic acid grafted cellulosic Luffa cylindrical fiber for the removal of dye and metal ions. *Carbohydr Polym* 98:1214–1221. <https://doi.org/10.1016/j.carbpol.2013.07.019>
- Hameed BH, Din ATM, Ahmad AL (2007) Adsorption of methylene blue onto bamboo-based activated carbon: Kinetics and equilibrium studies. *J Hazard Mater* 141:819–825. <https://doi.org/10.1016/j.jhazmat.2006.07.049>
- Han R, Zhang L, Song C et al (2010) Characterization of modified wheat straw, kinetic and equilibrium study about copper ion and methylene blue adsorption in batch mode. *Carbohydr Polym* 79:1140–1149. <https://doi.org/10.1016/j.carbpol.2009.10.054>
- Haque E, Jun JW, Jung SH (2011) Adsorptive removal of methyl orange and methylene blue from aqueous solution with a metal-organic framework material, iron terephthalate (MOF-235). *J Hazard Mater* 185:507–511. <https://doi.org/10.1016/j.jhazmat.2010.09.035>
- He X, Male KB, Nesterenko PN et al (2013) Adsorption and desorption of methylene blue on porous carbon monoliths and nanocrystalline cellulose. *ACS Appl Mater Interfaces* 5:8796–8804. <https://doi.org/10.1021/am403222u>
- Kannan N, Sundaram MM (2001) Kinetics and mechanism of removal of methylene blue by adsorption on various carbons: A comparative study. *Dye Pigment* 51:25–40. [https://doi.org/10.1016/S0143-7208\(01\)00056-0](https://doi.org/10.1016/S0143-7208(01)00056-0)
- Lehtonen J, Hassinen J, Kumar AA et al (2020) Phosphorylated cellulose nanofibers exhibit exceptional capacity for

- uranium capture. *Cellulose* 1:1–14. <https://doi.org/10.1007/s10570-020-02971-8>
- Lellis B, Fávoro-Polonio CZ, Pamphile JA, Polonio JC (2019) Effects of textile dyes on health and the environment and bioremediation potential of living organisms. *Biotechnol Res Innov* 3:275–290. <https://doi.org/10.1016/j.biori.2019.09.001>
- Luo X, Yuan J, Liu Y et al (2017) Improved Solid-Phase Synthesis of Phosphorylated Cellulose Microsphere Adsorbents for Highly Effective Pb²⁺ Removal from Water: Batch and Fixed-Bed Column Performance and Adsorption Mechanism. *ACS Sustain Chem Eng* 5:5108–5117. <https://doi.org/10.1021/acssuschemeng.7b00472>
- Ma H, Burger C, Hsiao BS, Chu B (2012) Nanofibrous micro-filtration membrane based on cellulose nanowhiskers. *Biomacromol* 13:180–186. <https://doi.org/10.1021/bm201421g>
- Mautner A, Maples HA, Kobkeatthawin T et al (2016) Phosphorylated nanocellulose papers for copper adsorption from aqueous solutions. *Int J Environ Sci Technol* 13:1861–1872. <https://doi.org/10.1007/s13762-016-1026-z>
- Noguchi Y, Homma I, Matsubara Y (2017) Complete nanofibrillation of cellulose prepared by phosphorylation. *Cellulose*. 24:1295–1305. <https://doi.org/10.1007/s10570-017-1191-3>
- Noguchi Y, Homma I, Watanabe T (2020) Properties of phosphorylated cellulose nanofiber dispersions under various conditions. *Cellulose* 27:2029–2040. <https://doi.org/10.1007/s10570-019-02922-y>
- Okita Y, Saito T, Isogai A (2010) Entire surface oxidation of various cellulose microfibrils by TEMPO-mediated oxidation. *Biomacromol* 11:1696–1700. <https://doi.org/10.1021/bm100214b>
- Oshima T, Kondo K, Ohto K et al (2008) Preparation of phosphorylated bacterial cellulose as an adsorbent for metal ions. *React Funct Polym* 68:376–383. <https://doi.org/10.1016/j.reactfunctpolym.2007.07.046>
- Rafatullah M, Sulaiman O, Hashim R, Ahmad A (2010) Adsorption of methylene blue on low-cost adsorbents: A review. *J Hazard Mater* 177:70–80
- Reid D, Laurence W, Mazzeno J (1949) Preparation and Properties of cellulose Phosphates. *Ind Eng Chem* 41:2828–2831
- Rol F, Sillard C, Bardet M et al (2020) Cellulose phosphorylation comparison and analysis of phosphorate position on cellulose fibers. *Carbohydr Polym* 229:115294. <https://doi.org/10.1016/j.carbpol.2019.115294>
- Schwarzenbach RP, Escher BI, Fenner K et al (2006) The challenge of micropollutants in aquatic systems. *Science* 313:1072–1077
- Segal L, Creely JJ, Martin AE, Conrad CM (1959) An Empirical Method for Estimating the Degree of Crystallinity of Native Cellulose Using the X-Ray Diffractometer. *Text Res J* 29:786–794. <https://doi.org/10.1177/004051755902901003>
- Sehaqui H, de Larraya UP, Liu P et al (2014) Enhancing adsorption of heavy metal ions onto biobased nanofibers from waste pulp residues for application in wastewater treatment. *Cellulose* 21:2831–2844. <https://doi.org/10.1007/s10570-014-0310-7>
- Sehaqui H, Mautner A, Perez De Larraya U et al (2016a) Cationic cellulose nanofibers from waste pulp residues and their nitrate, fluoride, sulphate and phosphate adsorption properties. *Carbohydr Polym* 135:334–340. <https://doi.org/10.1016/j.carbpol.2015.08.091>
- Sehaqui H, Michen B, Marty E et al (2016b) Functional cellulose nanofiber filters with enhanced flux for the removal of humic acid by adsorption. *ACS Sustain Chem Eng* 4:4582–4590. <https://doi.org/10.1021/acssuschemeng.6b00698>
- Sehaqui H, Spera P, Huch A, Zimmermann T (2018) Nanoparticles capture on cellulose nanofiber depth filters. *Carbohydr Polym* 201:482–489. <https://doi.org/10.1016/j.carbpol.2018.07.068>
- Sharma P, Kaur H, Sharma M, Sahore V (2011) A review on applicability of naturally available adsorbents for the removal of hazardous dyes from aqueous waste. *Environ Monit Assess* 183:151–195
- Sivaram NM, Gopal PM, Barik D (2018) Toxic waste from textile industries. In: *Energy from toxic organic waste for heat and power generation*. Elsevier, pp 43–54
- Srivastava N, Thakur AK, Shahi VK (2016) Phosphorylated cellulose triacetate-silica composite adsorbent for recovery of heavy metal ion. *Carbohydr Polym* 136:1315–1322. <https://doi.org/10.1016/j.carbpol.2015.10.047>
- Suflet DM, Chitanu GC, Popa VI (2006) Phosphorylation of polysaccharides: New results on synthesis and characterisation of phosphorylated cellulose. *React Funct Polym* 66:1240–1249. <https://doi.org/10.1016/j.reactfunctpolym.2006.03.006>
- Suflet DM, Popescu I, Pelin IM (2017) PREPARATION AND ADSORPTION STUDIES OF PHOSPHORYLATED CELLULOSE MICROSPHERES. *Cellulose Chem Technol* 51:23–34
- Youssef B, Soumia A, Mounir EA et al (2015) Preparation and properties of bionanocomposite films reinforced with nanocellulose isolated from moroccan alfa fibres. *Autex Res J*. <https://doi.org/10.1515/aut-2015-0011>
- Zhuang S, Wang J (2019) Removal of U(VI) from aqueous solution using phosphate functionalized bacterial cellulose as efficient adsorbent. *Radiochim Acta* 107:459–467. <https://doi.org/10.1515/ract-2018-3077>

Publisher's Note Springer Nature remains neutral with regard to jurisdictional claims in published maps and institutional affiliations.